

Chemical characterization and source analysis of water-soluble inorganic ions in PM_{2.5} from a plateau city of Kunming at different seasons



Wei Guo^{a,b}, Zhongyi Zhang^{a,b}, Nengjian Zheng^{a,b}, Li Luo^{a,b}, Huayun Xiao^{a,c,*}, Hongwei Xiao^{a,b,*}

^a Jiangxi Province Key Laboratory of the Causes and Control of Atmospheric Pollution, East China University of Technology, Nanchang 330013, China

^b College of Water Resources and Environmental Engineering, East China University of Technology, Nanchang 330013, China

^c State Key Laboratory of Environmental Geochemistry, Institute of Geochemistry, Chinese Academy of Sciences, Guiyang 550002, China

ARTICLE INFO

Keywords:

PM_{2.5}

Water-soluble inorganic ions (WSIIs)

Source identification

Seasonality

Kunming

ABSTRACT

Water-soluble inorganic ions (WSIIs) in PM_{2.5} from different cities have been studied in previous studies. However, the studies of WSIIs in plateau cities are relative deficient. Due to differences in topography, climate and emission sources, the WSIIs characteristics of plateau cities are expected to be different. Here, we determined the concentrations of WSIIs (SO_4^{2-} , NO_3^- , NH_4^+ , Ca^{2+} , Mg^{2+} , Na^+ , K^+ , F^- , Cl^- , NO_2^-) in PM_{2.5} from different seasons of Kunming, a typical plateau city in southwest China. The data will improve our understanding of the chemical characterization and source of PM_{2.5} in plateau environment. Our results showed that the secondary aerosols were the main pollutants (contributing > 50% to PM_{2.5}) in PM_{2.5} of Kunming, which mainly from coal combustion, agricultural activities and vehicle exhaust. Seasonally, high volatility of the NO_3^- and NH_4^+ and washout effects of rainfall in hot months (wet seasons) were favorable for the decreased of pollutants, while high emission, poor dispersion conditions and low removal rate could lead to the increased of pollutants in cold months (dry seasons). It suggested that adequate NH₃ and intense solar radiation promotes the photochemical reactions of SO₂, NO_x and NH₃ to form NH_4HSO_4 , $(\text{NH}_4)_2\text{SO}_4$ and NH_4NO_3 . High temperature in hot months would promote the volatilization of NH_4NO_3 in Kunming.

1. Introduction

PM_{2.5} generally defined as those particles with an aerodynamic diameter of 2.5 μm or less, which also known as fine particulate matter and is the major cause of haze in most areas (Yuan et al., 2006; Dai et al., 2013). The PM_{2.5} include primary particles and secondary particles, the primary particles are emitted directly from a source, such as soil dust from fields, highway and construction sites, biological emissions from fires, sea salt from the ocean, and the secondary particles are formed in complicated reactions of the atmospheric gases, such as SO₂, NO_x and NH₃ which are emitted from vehicles, coal-fired power plants, industries and farms (Dai et al., 2013; Xiao et al., 2016). The PM_{2.5} has been paid more attention in recent decades due to its direct and indirect impacts on air quality and atmosphere visibility (Yuan et al., 2006; Liu et al., 2017), radiative balance (Gao et al., 2011; Contini et al., 2014) and nutrient deposition (Xiao et al., 2016). Especially, the PM_{2.5} can cause serious health problems (Li et al., 2013; He et al., 2017). With the rapid development of industrialization and urbanization, the contributions of vehicle exhaust emission, industrial gaseous pollutants and

coal combustion emission to aerosol particles increase rapidly in China (Wang et al., 2015), consequently, the serious air pollutions, especially PM_{2.5} pollution events were occurred frequently in some Chinese cities in recent years (He et al., 2017). The PM_{2.5} can be made up of complex chemical components, and in these components, water-soluble inorganic ions (WSIIs) such as sulfate, nitrate and ammonium (SNA) are the important components which can account for 20% to 70% or even more 70% of the PM_{2.5} mass (Dai et al., 2013; He et al., 2017). WSIIs have effects on the hydroscopic nature (Shen et al., 2009; He et al., 2017) and acidity of PM_{2.5} (Gao et al., 2011), it also play an important role in degrading the visibility (Yuan et al., 2006) and accelerating the formation of PM_{2.5} (Zhou et al., 2018). Therefore, investigating the WSIIs characteristics is an effective way for us understanding the sources, behaviors and formation mechanism of PM_{2.5} (Wang et al., 2015).

Many studies have been conducted in China, attempting to characterize the sources and formation process of PM_{2.5} pollution by investigating the composition of WSIIs. Most of them were focused on the cities where the PM_{2.5} pollution were relatively more serious, such as

* Corresponding authors at: Jiangxi Province Key Laboratory of the Causes and Control of Atmospheric Pollution, East China University of Technology, Nanchang 330013, China.

E-mail addresses: xiaohuayun@ecit.cn (H. Xiao), xiaohw@ecit.cn (H. Xiao).

Jing-Jin-Ji region (Zhao et al., 2013; Meng et al., 2016; Yang et al., 2017), Yellow River Basin region (Shen et al., 2009; He et al., 2017; Zhou et al., 2018), Yangtze River Delta region (Wang et al., 2006; Wang et al., 2016; Xu et al., 2017a; Zhang et al., 2018), Pearl River Delta region (Tao et al., 2012; Dai et al., 2013; Zhou et al., 2016), and coastal region (Zhao et al., 2011; Xu et al., 2012). However, the studies of WSIs in plateau cities of China are relative deficient, where the PM_{2.5} pollutions are relatively light. Moreover, most previous studies were focused on some certain periods and seasons or pollution events, the studies of WSIs in PM_{2.5} at four seasons around one year are also scarce.

Kunming is a plateau city with high elevation (1500 to 1800 m) and low latitude (24°23'N to 26°22'N). It has typical plateau monsoon climate characteristics and holds two distinct seasons, the wet season from May to October and dry season from November to next April. The wet season accounts for 85% of the annual rainfall, and the dry season has intense solar radiation with an average of 20 days of sunshine in a month (Shi et al., 2016; Zhu et al., 2016). These individual topographic and climatic features are different from other cities of China. It is expected that aerosol properties in dry season may be different from that of wet season, and the aerosol properties in Kunming may be different from those in other cities of China (Shi et al., 2016; Zhu et al., 2016). In recent years, with the development of tourism and the economy, the impact of human activities on air quality and living environment have intensified in Kunming, which has been experiencing elevated levels of PM_{2.5} pollution (Bi, 2015; Li et al., 2017). However, there are less comprehensive studies on PM_{2.5} in Kunming up to date (Shi et al., 2016; Zhu et al., 2016), especially the study about WSIs in PM_{2.5} at different seasons. This study is expected to provide valuable data for better understanding the chemical characterization and source of PM_{2.5} in plateau environment.

This research is aimed to better understand the chemical composition and potential sources of PM_{2.5} in Kunming in different seasons, then discuss the different formation mechanisms of PM_{2.5} under different urban background. In this study, daily collected WSIs in PM_{2.5} were measured in Kunming from the September 1, 2017 to the August 31, 2018 (last one year), and seasonal variations of WSIs in PM_{2.5} were also discussed. In addition, a source apportionment receptor model, positive matrix factorization (PMF) was used to help identifying the potential sources of PM_{2.5} in different seasons.

2. Material and methods

2.1. Study area and sampling site

Kunming is (102°10'E to 103°40'E, 24°23'N to 26°22'N) located in the middle of the Yunnan-Guizhou Plateau in southwest of China, with the altitude is 1500 to 1800m, which is the capital city of Yunnan Province (Fig. 1). It belongs to the low-latitude plateau mountain monsoon climate, with intense solar radiation and optimum temperature (0 °C to 29 °C, average 16.5 °C). In this study, we selected Kunming University of Science and Technology (KUST) (Lianhua Campus) as the sampling site (102° 42'E, 25°04'N) (on the rooftop of Faculty of Land Resource Engineering in KUST) for collecting PM_{2.5} samples. The sampling site is located in the northwest of Kunming where is the mixed district of commerce, traffic and resident (Fig. 1).

2.2. Sample collection and WSIs analysis

PM_{2.5} samples were collected on quartz fiber filters (8 × 10 in., Tissuquartz™ Filters, Washington, USA) by using a specific high flow rate ($1.05 \pm 0.03 \text{ m}^3 \cdot \text{min}^{-1}$) KC-1000 sampler (Laoshan Institute for Electronic Equipment, Qingdao, China). All filters were pre-baked at 450 °C for 4 h before sampling to remove residual organic contamination. In this study, a total of 346 daily PM_{2.5} samples were collected from September 1, 2017 to August 31, 2018, and the sampling time was

from 9 a.m. to 9 a.m. of next day. All collected samples were stored in a refrigerator at -20 °C until analysis in the laboratory.

In the laboratory, one eighth filters were cut and placed in a clean 50 mL Nalgene tube with additional 50 mL ultrapure water. They were washed for 30 min by ultrasonic vibration and shaken for 30 min on a shaker, and then centrifugalize for another 10 min. The supernatant was filtered using syringe filter with a 0.22μm microporous membrane (reference Xiao et al., 2016). The filtrate stored in a refrigerator at -20 °C until chemical analyses.

We using ion chromatographic (Dionex Aquion (AQ)™, Thermo Scientific™, USA) to detect inorganic ion concentration include SO₄²⁻, NO₃⁻, NH₄⁺, Ca²⁺, Cl⁻, Mg²⁺, Na⁺, K⁺ and F⁻. The detection limit of them were 11.50 μg·L⁻¹, 21.60 μg·L⁻¹, 1.21 μg·L⁻¹, 0.09 μg·L⁻¹, 5.10 μg·L⁻¹, 2.47 μg·L⁻¹, 0.001 μg·L⁻¹, 1.77 μg·L⁻¹ and 3.80 μg·L⁻¹, respectively.

2.3. Meteorological and air quality data collection

Gaseous pollutants (PM_{2.5}, PM₁₀, SO₂, NO₂, O₃ and CO) concentrations were obtained from China Air Quality Online Monitoring and Analysis Platform (<https://www.aqistudy.cn/>). Temperature (T), relative humidity (RH), wind speed (WS) and wind direction (WD) data was collected in the Global Weather and Climate Information Network (<http://www.weatherandclimate.info/>).

2.4. Positive matrix factorization (PMF) model analysis

PMF is widely used and effective source apportionment receptor model (Hien et al., 2004; Tiwari et al., 2013). In this study, the EPA (United States Environmental Protection Agency) PMF 5.0 was used to determine source apportionment of WSIs.

2.5. Calculation of sulfur oxidation ratio (SOR) and nitrogen oxidation ratio (NOR)

SOR and NOR are generally used to infer the degree of atmospheric secondary transformation of SO₂ and NO₂ to SO₄²⁻ and NO₃⁻. The SOR and NOR could be calculated by the following equations (Khoder, 2002; Zhou et al., 2018):

$$\text{SOR} = [\text{SO}_4^{2-}] / ([\text{SO}_4^{2-}] + [\text{SO}_2]) \quad (1)$$

$$\text{NOR} = [\text{NO}_3^-] / ([\text{NO}_3^-] + [\text{NO}_2]) \quad (2)$$

where the [SO₄²⁻], [SO₂], [NO₃⁻] and [NO₂] are the molar concentrations (μmol·m⁻³) in PM_{2.5} and gas phase.

3. Results

3.1. Meteorological records and air quality data

During the sampling period, the wind speed was in the range of 0.5 to 5.1 m·s⁻¹ (average 2.3 m·s⁻¹), and it was relatively high in spring (Mar, Apr and May). The dominant wind directions are south, southwest and west (Fig. 1 and Fig. 2a). The rainfall was in the range of 0.1 to 64.1 mm, and was mainly concentrated in May to October (wet season) in sampling period. The pH value of rainfall was 5.9 to 8.9 (Kunming Environmental Statement, 2017 and 2018). The temperature and RH were -1.3 to 22.9 °C (average 16.0 °C) and 39.3 to 93.5% (average 70.8%), respectively (Fig. 2b). In gaseous pollutants, the NO₂ (average 34 μg·m⁻³), SO₂ (average 15 μg·m⁻³), O₃ (average 82 μg·m⁻³) and CO (average 1.0 mg·m⁻³) were kept medium concentration (Fig. 2c and d) and close to other developed cities of china, e.g. Beijing, Shanghai, Guangzhou (<https://www.aqistudy.cn/>). The PM_{2.5} and PM₁₀ were from 8 to 101 μg·m⁻³ (average 31 μg·m⁻³) and from 17 to 174 μg·m⁻³ (average 58 μg·m⁻³), respectively. The PM_{2.5} concentrations were generally lower than most of cities in China (<https://www.aqistudy.cn/>

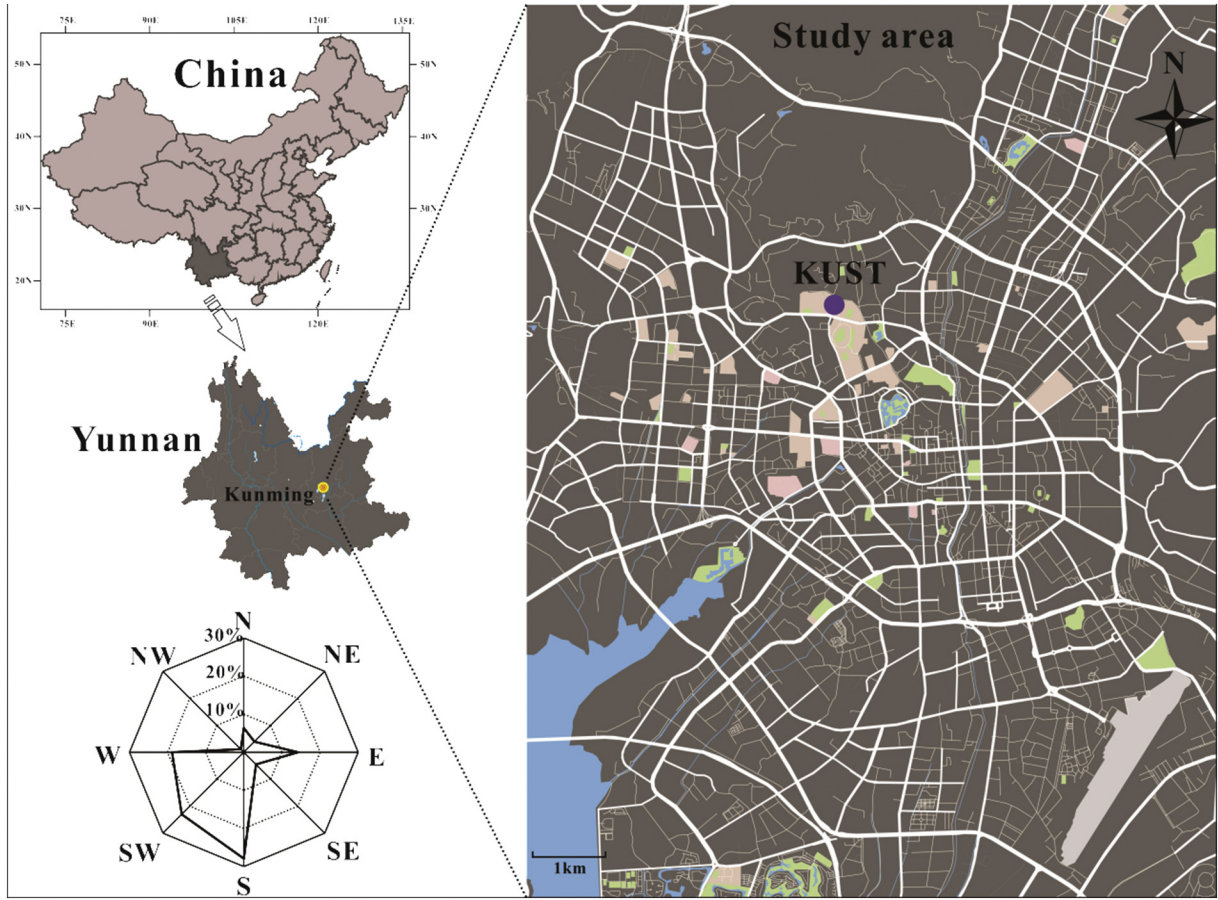


Fig. 1. Map of the sampling site, including the position of the Yunnan province and urban areas of Kunming.

). It can be seen that high PM_{2.5} and PM₁₀ concentration were accompanied by high levels of NO₂ and SO₂ (Fig. 2d).

3.2. WSII concentration in PM_{2.5}

The main WSII in PM_{2.5} include SO₄²⁻, NO₃⁻, NH₄⁺, Ca²⁺, Mg²⁺, Na⁺, K⁺, F⁻ and Cl⁻, and its total concentrations for all samples were from 3.46 to 46.20 $\mu\text{g m}^{-3}$, average 15.59 $\mu\text{g m}^{-3}$ (Fig. 2e), which occupied about 15.7 to 99. 1% of PM_{2.5} mass (average 51.5%). SO₄²⁻ (43.9%) and NO₃⁻ (15.2%) were the most abundant anion, NH₄⁺ (16.2%) and Ca²⁺ (16.0%) was the most abundant cation. The proportion of Cl⁻ (3.3%), K⁺ (2.8%), F⁻ (1.2%), Mg²⁺ (0.8%) and Na⁺ (0.6%) were relatively low compared to the other ions. The change of WSII concentrations were corresponded well with the variation of PM_{2.5} (Fig. 2d and e).

Seasonally, the WSII concentrations were relatively high in cold months (Nov, Dec, Jan, Feb, Mar and Apr) (Fig. 3) when the temperature and rainfall were low (Fig. 2b), while were relatively low in hot months (May, Jun, Jul, Aug, Sep and Oct) (Fig. 3) when the temperature and rainfall were high (Fig. 2b). It's to be noted that the concentration of K⁺ were relative high in February 2018 (Fig. 3e). The change of SO₄²⁻ and NO₃⁻ were consistent with SOR and NOR (Fig. 3a and b).

3.3. Results of PMF model analysis

Based on the PMF model, six mainly factors (potential sources) were identified and quantified in Kunming. It showed that the factor 1 contributed 76.4% of NO₃⁻, factor 2 contributed 68.7% of Cl⁻, factor 3 contributed 60.1% of Ca²⁺, 38.5% of Mg²⁺ and 55.5% of Na⁺, factor 4 contributed 81.6% of F⁻, factor 5 contributed 91.0% of K⁺ and 34.3%

of Mg²⁺, factor 6 contributed 69.0% of SO₄²⁻ and 72.6% of NH₄⁺ from contribution distribution of factors to ion species (Table 1 and Fig. S1). The factor 1 to factor 6 were mainly characterised by NO₃⁻ (factor 1), Cl⁻ (factor 2), Ca²⁺, Mg²⁺ and Na⁺ (factor 3), F⁻ (factor 4), K⁺ and Mg²⁺ (factor 5), SO₄²⁻ and NH₄⁺ (factor 6), respectively, and their contribution proportion to PM_{2.5} were 27.1%, 7.6%, 24.8%, 3.4%, 6.8% and 30.4%, respectively (Table 1). Seasonally, the variation of contributions for different factors were consistent with the WSII concentrations that the relative contributions were relatively high in cold months, while were low in hot months (Fig. 4).

3.4. Correlations of WSII

The linear correlations of different anions and cations (microgram-equivalents concentrations, μeq vs. μeq) in PM_{2.5} were analysed. As showed that NH₄⁺ was strongly linear correlated with SO₄²⁻, and the slopes of linear equations were lower than 1 in hot months, while > 1 in cold months (Fig. 5a). We used the correlations between excess NH₄⁺ (excess [NH₄⁺] = ([NH₄⁺] / [SO₄²⁻] - 1.5) \times [SO₄²⁻]) and NO₃⁻ concentration to show the reaction between NH₃ and HNO₃ (Pathak et al., 2008; Zhou et al., 2018). In our result, most of the samples were NH₄⁺ rich (excess NH₄⁺ > 0), and in NH₄⁺-rich conditions, the NO₃⁻ concentration increased with excess NH₄⁺ (Fig. 5b). The [SO₄²⁻ + NO₃⁻] was strongly linear correlated with [NH₄⁺], and the slopes of linear regressions equation between [SO₄²⁻ + NO₃⁻] and [NH₄⁺] was lower than 1 (Fig. 5c). Meanwhile, the cations (NH₄⁺ + Ca²⁺ + Mg²⁺ + Na⁺ + K⁺) equivalent concentration (CE) were linear related to anions (SO₄²⁻ + NO₃⁻ + F⁻ + Cl⁻) equivalent concentration (AE), and most of samples were below (lower than) the 1:1 line (Fig. 5d).

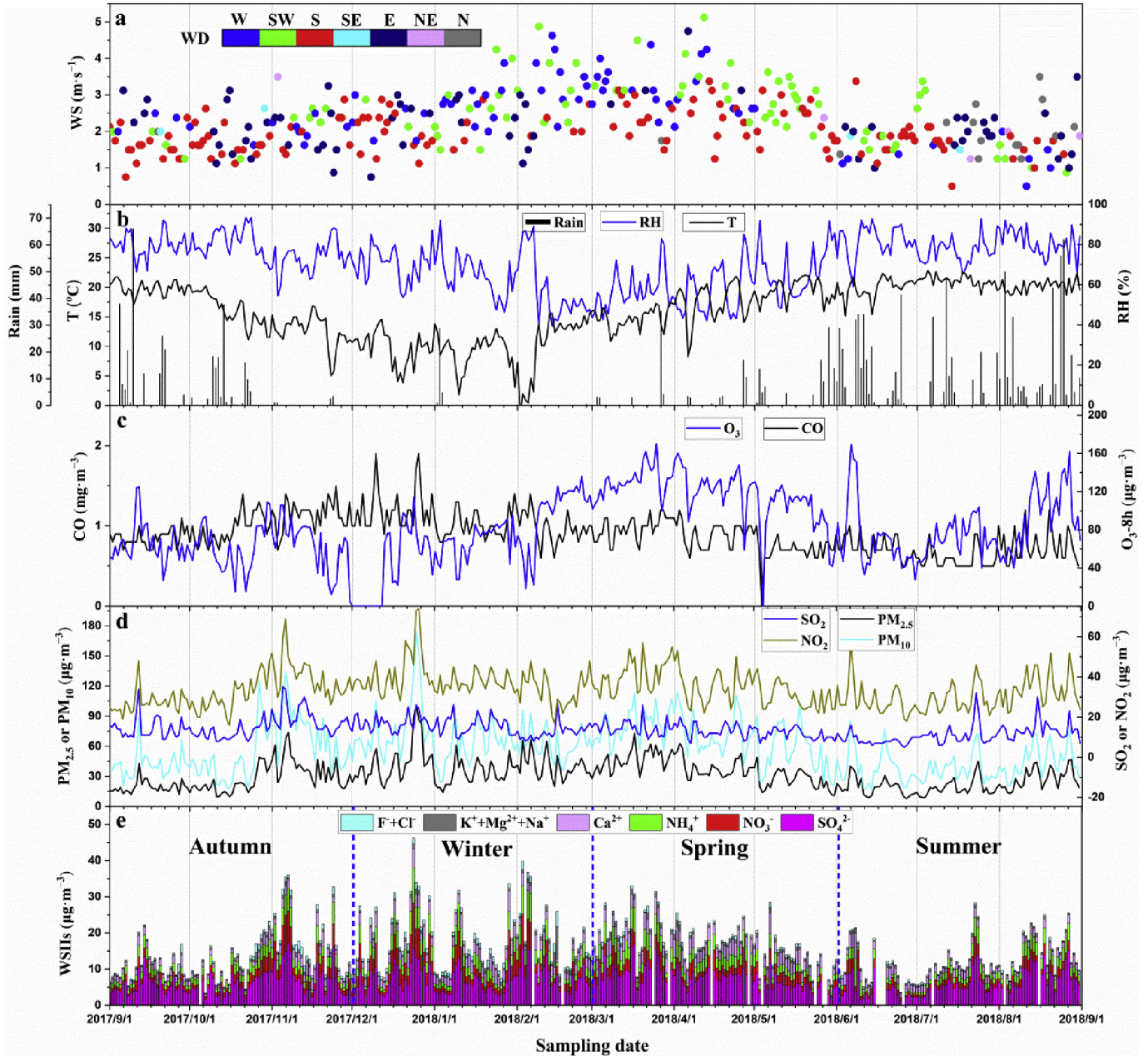


Fig. 2. Meteorological and gaseous pollutants records, $\text{PM}_{2.5}$ (PM_{10}) and WSIs concentrations in sampling periods.

4. Discussion

4.1. The influence of meteorological conditions and ambient gaseous pollutants to the $\text{PM}_{2.5}$ concentration

Meteorological conditions have important effects on the concentrations of air pollutants. The first important meteorological factor is wind speed and wind direction (Xu et al., 2017b). In our study of Kunming, the wind speed was higher than $3 \text{ m}\cdot\text{s}^{-1}$ in most of time, and there was no significant correlation between wind speed and $\text{PM}_{2.5}$ or PM_{10} , suggesting that the transport of pollutants relate to wind speed from the source regions to the Kunming might be weakly. In December 24 to 27, 2017, when the $\text{PM}_{2.5}$ concentration was relative high (83 to $101 \mu\text{g}\cdot\text{m}^{-3}$) in hazy day, the wind speed (1.1 to $1.9 \text{ m}\cdot\text{s}^{-1}$) was relative lower than the mean level ($2.3 \text{ m}\cdot\text{s}^{-1}$), which confirms that low wind speed may be not favor the diffusion of pollutants. Another important meteorological factor is the atmospheric RH. High

concentration of aerosol liquid water would dissolve more pollutants and accelerate chemical reaction (Boreddy et al., 2016; Xu et al., 2017b). There was no significant correlation between RH and $\text{PM}_{2.5}$ or PM_{10} in our results, which suggested that the RH had little effect on the aerosol concentration in Kunming. In addition, low air temperatures before the haze episodes would favor the partitioning of semi-volatile components and ammonium into the particle phase, which further exacerbating air pollution (Xu et al., 2017b). In our results, the temperature was 5.5 to 12.3°C in hazy day in December 24 to 27, 2017, which was higher than the temperature of a few days ago (3.9 to 8.1°C) (Fig. 2b). This may confirm that low air temperatures before the haze episodes are promote the formation of pollutants. Gaseous pollutants also have important effects on the concentrations of air pollutants. The variation of $\text{PM}_{2.5}$ were coincide with the variation of NO_2 and SO_2 (Fig. 2d) and $\text{PM}_{2.5}$ were correlated with NO_2 and SO_2 (R^2 is 0.76 and 0.43 , respectively), which be attributing to that NO_2 and SO_2 are the precursor gases that could form sulfates and nitrates containing in

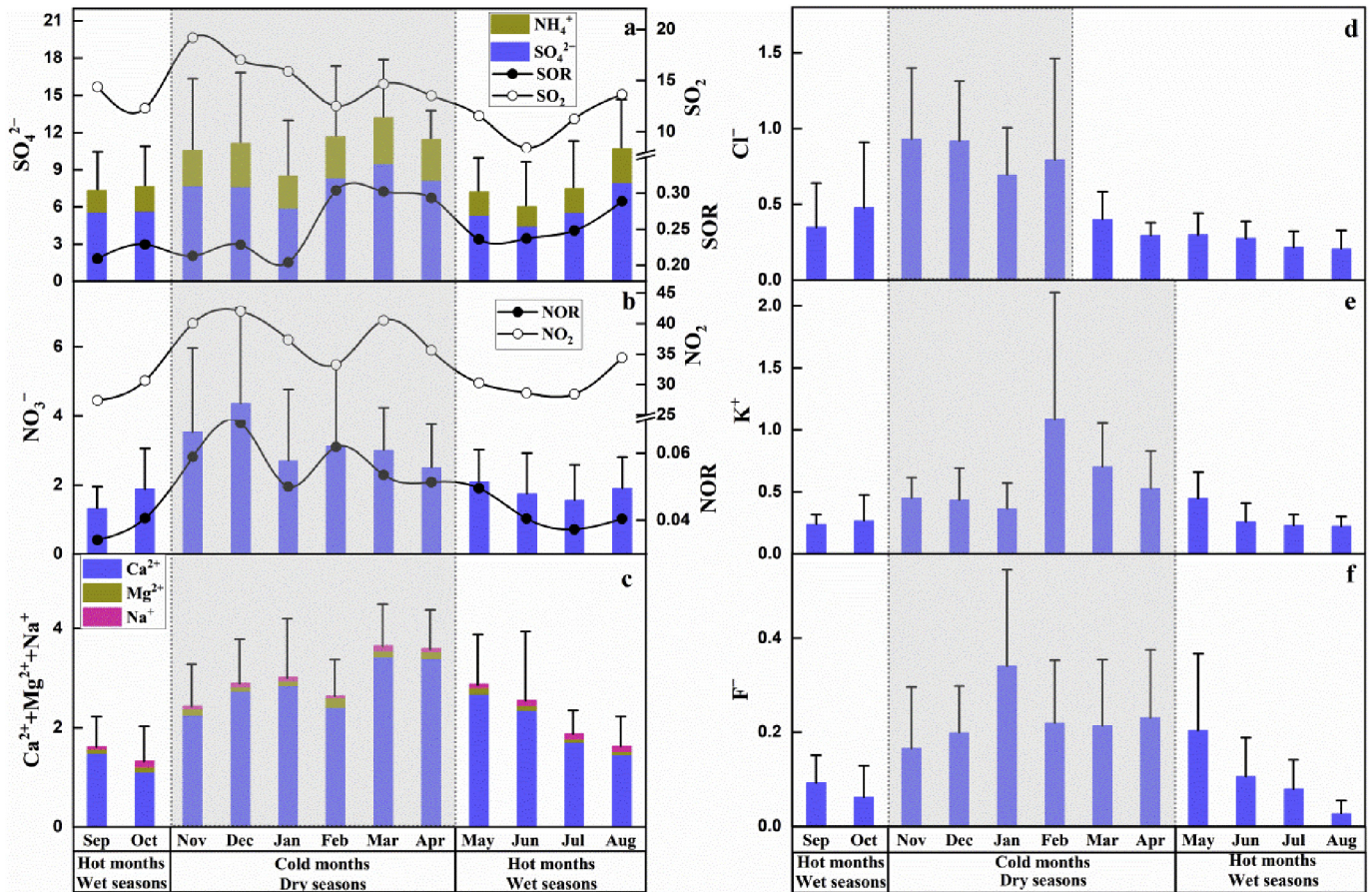


Fig. 3. Average WSII concentrations in different months. The unit of WSII and gaseous pollutants are $\mu\text{g}\cdot\text{m}^{-3}$.

Table 1

Relative contribution (%) of factors (potential sources) to different ions and $\text{PM}_{2.5}$ in Kunming over one year, based on PMF model.

Sources (%)	Factor	SO_4^{2-}	NO_3^-	NH_4^+	Ca^{2+}	Mg^{2+}	Na^+	K^+	F^-	Cl^-	$\text{PM}_{2.5}$
Secondary aerosols from vehicle exhaust	Factor 1	14.2	76.4	22.7	20.3	1.0	0.1	9.0	–	26.7	27.1
Coal combustion	Factor 2	–	4.0	0.4	–	5.6	16.6	–	11.9	68.7	7.6
Soil dust	Factor 3	11.2	14.1	–	60.1	38.5	55.5	–	1.3	–	24.8
Industry	Factor 4	–	5.5	2.7	17.2	6.0	1.2	–	81.6	–	3.4
Biomass burning	Factor 5	5.6	–	1.6	1.6	34.3	0.3	91.0	2.8	4.5	6.8
Secondary aerosols from coal combustion and agricultural activities	Factor 6	69.0	–	72.6	0.8	14.7	26.3	0.1	2.4	–	30.4

$\text{PM}_{2.5}$ (Shen et al., 2009; Li et al., 2013).

4.2. Source identification of WSII

4.2.1. The source of SO_4^{2-} , NO_3^- and NH_4^+ (SNA)

SNA were the most important ions in $\text{PM}_{2.5}$ in Kunming, and SO_4^{2-} ions exhibited the highest annual mean concentration and much higher than NO_3^- and NH_4^+ . In generally, most SO_4^{2-} is formed via the oxidation of SO_2 , which is produced primarily by coal combustion and some biomass burning (Wang et al., 2006; Deng et al., 2016). Particulate-related NO_3^- is formed primarily by the oxidation of NO_x (nitrogen oxides), which is derived primarily from vehicle exhaust (Wang et al., 2006; Deng et al., 2016). The concentration of SO_2 was less than NO_2 , the SOR (> 0.1) and SO_4^{2-} concentrations were much more than NOR (lower than 0.1) and NO_3^- , respectively, which indicates that the secondary formation of SO_4^{2-} from SO_2 strongly occurred in Kunming compared to that of NO_3^- from NO_2 (Khoder, 2002; Zhao et al., 2011). The NH_4^+ is formed primarily through gas/aqueous-phase reactions between NH_3 and acidic species (e.g., HCl , HNO_3 and H_2SO_4), which is mainly from agricultural activities, such as the application of nitrogen

fertilizers and the volatilization of livestock waste (Zhao et al., 2011; Zhang et al., 2018).

4.2.2. The source of Ca^{2+} and Mg^{2+}

Ca^{2+} was another important ion in Kunming, which was the fourth highest concentration WSII. It has been suggested that higher concentration of Ca^{2+} than Mg^{2+} and a low $\text{Mg}^{2+}/\text{Ca}^{2+}$ ratio of 0.09 would indicate the Ca^{2+} and Mg^{2+} are from soil dust (He et al., 2017). The $\text{Mg}^{2+}/\text{Ca}^{2+}$ ratio increase would indicate the Ca^{2+} and Mg^{2+} are affected by anthropogenic sources, such as coal usage and industry, et al. (Zhao et al., 2011; Li et al., 2013). The $\text{Mg}^{2+}/\text{Ca}^{2+}$ is approximately 0.12 and 0.17 in sea salt desert region aerosol, respectively (Deng et al., 2016). In our results, the concentration of Ca^{2+} was much more than Mg^{2+} , and average $\text{Mg}^{2+}/\text{Ca}^{2+}$ ratio was about 0.09 (0.02 to 1.91), this may indicate that the Ca^{2+} and Mg^{2+} are mainly from soil dust.

4.2.3. The source of Cl^- , K^+ and F^-

The proportion of Cl^- and K^+ was lower than that of SNA and Ca^{2+} . In fine particles, Cl^- and K^+ has multi-sources including biomass

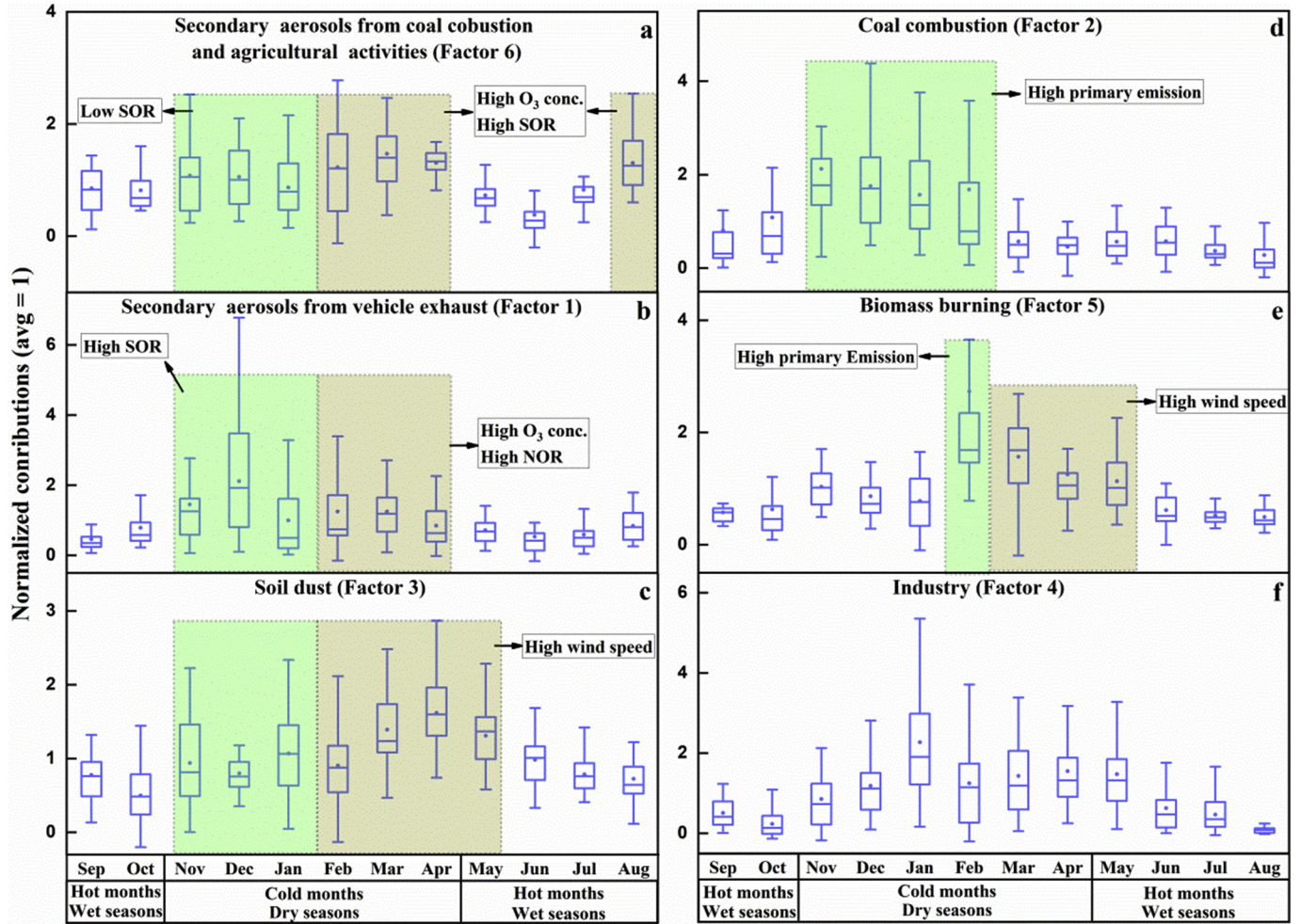


Fig. 4. Seasonal normalized contributions of factors to $\text{PM}_{2.5}$ in Kunming by PMF model. For each box plot of normalized contributions, the centerline represents the median, the box encompasses the 25th to 75th percentiles, and the bar denotes the 5th and 95th percentiles.

burning, coal combustion and sea-salts, et al. (Shen et al., 2009; Zhao et al., 2011; Liu et al., 2017). It has been suggested that the abundance of K^+ and low Cl^-/K^+ ratios, and strong correlation between K^+ and Cl^- can serve as a diagnostic tracer for biomass burning source of K^+ (Gao et al., 2011; He et al., 2017; Wang et al., 2017). In our results, the concentrations of K^+ was closed to Cl^- (Fig. 3d and e), K^+ and Cl^- were weakly correlated ($R^2 = 0.38$), which indicating that K^+ may be partially contributed from biomass burning. Some research suggests soil and displayed of fireworks could also contribute to K^+ in $\text{PM}_{2.5}$ (Zhao et al., 2011; He et al., 2017). The Cl^-/Na^+ was 16.7 which much more than that of sea water (about 1.8, reference Moller, 1990; Contini et al., 2014), which indicates that sea-salt contribution of Cl^- and Na^+ might be neglected, and coal combustion may be important source to Cl^- . For soluble F^- in $\text{PM}_{2.5}$, some research suggest aluminum and glass industries are the main contributor for F^- , soil and decomposition of living organisms could also contribute to F^- (Kalinic et al., 1997; Zhao et al., 2011). There are some aluminum industries (such as Yunnan Aluminum Corporation Ltd) and glass works close to the sampling sites in Kunming, which may be the main contributor for F^- .

4.2.4. Quantitative source apportionment of WSIs by PMF model

Main six potential sources for WSIs were identified by PMF model, and these six sources (factors) were characterised by NO_3^- (factor 1), Cl^- (factor 2), Ca^{2+} , Mg^{2+} and Na^+ (factor 3), F^- (factor 4), K^+ and Mg^{2+} (factor 5), SO_4^{2-} and NO_3^- (factor 6), respectively (Table 1 and Fig. S1). Referenced to the different ion sources in Kunming as discussed in Sections 4.2.1 to 4.2.3, the main six potential sources are

representing the contribution of secondary aerosols from vehicle exhaust, coal combustion, soil dust, industry emissions, biomass burning and secondary aerosols from coal combustion and agricultural activities, and the contribution proportion to $\text{PM}_{2.5}$ were 27.1%, 7.6%, 24.8%, 3.4%, 6.8% and 30.4%, respectively (Table 1). In these sources, secondary aerosols that from coal combustion (SO_4^{2-}) and agricultural activities (NH_4^+) and vehicle exhaust (NO_3^-) are the main sources of $\text{PM}_{2.5}$ in Kunming, which contributing > 50% to $\text{PM}_{2.5}$.

4.3. Seasonal variation of WSIs sources

The results of PMF analysis showed that the normalized contributions of potential sources were relatively high in cold months and low in hot months (Fig. 4). This is in accordance well with the seasonal variation of WSIs concentrations (Fig. 3). In generally, this variation in WSIs concentrations and contributions are mainly related to seasonal climate change in Kunming. In hot months (wet season), the temperature and rainfall are relatively high (Fig. 2b), high volatility of the SNA (NH_4NO_3) and washout effects of rainfall on ions could lead to the lower concentrations and contributions (Zhao et al., 2011; Shi et al., 2016). Conversely, as the temperature and rainfall decrease in cold months (dry season), the dispersion conditions are poor, and the volatility and ion removal rate are reduced, which could result in the higher concentration and contributions in these months (Xu et al., 2017b; Zhou et al., 2018).

What's more, other reasons might also lead to the change of concentration and contributions in different months. For example, the

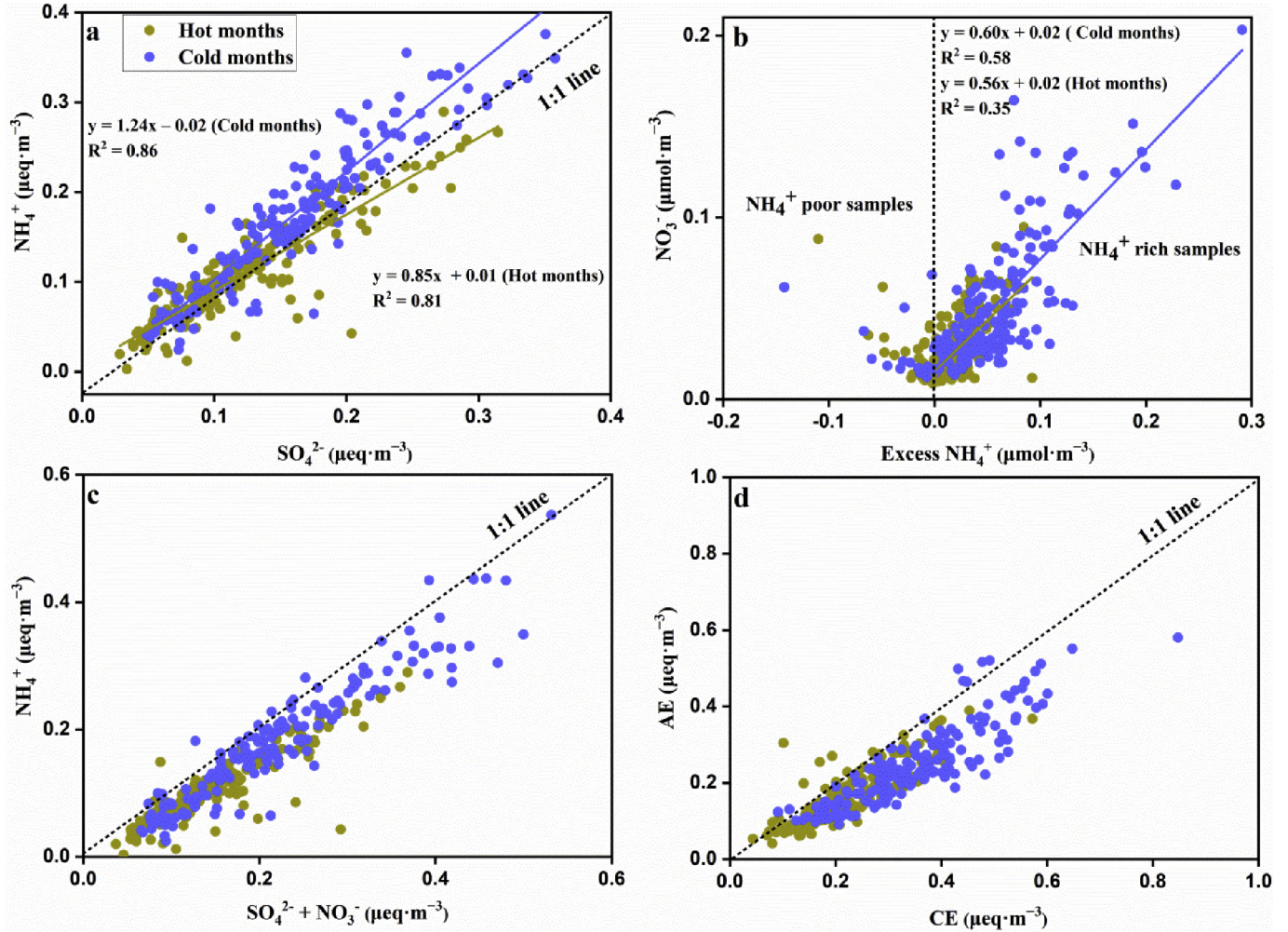


Fig. 5. Linear correlations of different anions and cations (microgram-equivalents concentrations, μeq vs. μeq) in $\text{PM}_{2.5}$.

increased transformation efficiency of SO_2 and NO_2 are also responsible for the high contributions of secondary particles (SO_4^{2-} , NH_4^+ and NO_3^-) in cold months (Fig. 4a and b), as both SOR and NOR are relatively high (Fig. 3a and b) in these months. In November, December and January, when the contributions of secondary particles from coal combustion and agricultural activities were high (Fig. 4a), the SOR was low (Fig. 3a), which may indicate that the non-secondary (primary emission) SO_4^{2-} were increased in these months. It could be seen that since the O_3 concentration (Fig. 2b) and SOR (Fig. 3a) were both high in August, the contributions of secondary particles from coal combustion and agricultural activities were also high in this month (Fig. 4a), although the removal effects of SNA existed in this month. High wind speed in February, March, April and May (Fig. 2a) could also result in the increased of soil dust sources (Fig. 4c). The increased of coal use for domestic heating and cooking in November, December, January and February also contributed to the high contributions of coal combustion (Fig. 5d). The contributions of biomass burning were high in February (Fig. 4e) which corresponding to the high K^+ and Mg^{2+} in February (Fig. 3e and c). Especially in February 16, 2018 that was the traditional Chinese New Year's Eve, the concentration of K^+ and Mg^{2+} were 7.86 and $1.01 \mu\text{g}\cdot\text{m}^{-3}$, respectively, which were the highest values in sampling period. This result may cause by displayed of fireworks and firecrackers. During the Chinese New Year holiday in February, especially Chinese New Year's Eve, people displayed a large amount of fireworks and firecrackers to celebrate the festival, which had an impact on the atmosphere. Previous studies had also reported that the displayed of fireworks could make the high Mg^{2+} and K^+ level in the

atmosphere (Shen et al., 2009). When the wind speed was high in spring (February March and April), the K^+ from soil dust was increased, which could cause the high contributions of biomass burning in spring (Fig. 4c).

4.4. Chemical forms of WSII in $\text{PM}_{2.5}$

NH_4^+ was strongly linear correlated with SO_4^{2-} in four seasons (Fig. 5a), which had been reported by many studies (Li et al., 2013; Liu et al., 2017), suggesting NH_4HSO_4 or $(\text{NH}_4)_2\text{SO}_4$ were the main existence form of NH_4^+ and SO_4^{2-} . The NH_4HSO_4 or $(\text{NH}_4)_2\text{SO}_4$ was primarily produced via the homogeneous reactions between the NH_3 and H_2SO_4 . The slopes of linear equations between NH_4^+ and SO_4^{2-} were lower than 1 in hot months, while > 1 in cold months. This may be attributed to the different equivalent ratios of NH_4^+ to SO_4^{2-} in NH_4HSO_4 (0.5) and $(\text{NH}_4)_2\text{SO}_4$ (1.0), respectively (He et al., 2017; Zhou et al., 2018). It could be inferred that both NH_4HSO_4 and $(\text{NH}_4)_2\text{SO}_4$ were the existence form of NH_4^+ and SO_4^{2-} in hot months when the temperature and RH were relative high, while $(\text{NH}_4)_2\text{SO}_4$ was the main existence form in cold months when the temperature and RH were relative low.

Both H_2SO_4 and HNO_3 could react with NH_3 to form salts (Zhou et al., 2018). However, NH_3 is preferential to react with H_2SO_4 to form NH_4HSO_4 or $(\text{NH}_4)_2\text{SO}_4$, and if NH_3 is enough for H_2SO_4 , the excess NH_3 could react with HNO_3 to form NH_4NO_3 (Pathak et al., 2008; Zhou et al., 2018). In this study, most of the samples were NH_4^+ rich (excess $\text{NH}_4^+ > 0$), and the NO_3^- concentration increased with excess NH_4^+

(Fig. 5b). This result confirmed that NO_3^- is primarily produced via the reaction between the NH_3 and HNO_3 , and NH_4NO_3 is the main existence form of NH_4^+ and NO_3^- . The formation of NO_3^- in NH_4^+ -poor samples (excess $\text{NH}_4^+ < 0$) cannot be explained by the homogeneous gas-phase mechanism, which may be associated with crustal species in $\text{PM}_{2.5}$ and hydrolysis of N_2O_5 (Pathak et al., 2008; Li et al., 2013). The volatilization of NH_4NO_3 in high temperature condition may be the reason for the lower correlation coefficient between excess NH_4^+ and NO_3^- in hot months (Fig. 5b) (He et al., 2017; Wang et al., 2017). This is in accordance with the discussion in Section 4.3.

The $[\text{SO}_4^{2-} + \text{NO}_3^-]$ was strongly linear correlated with NH_4^+ , and the slopes of linear regressions equation was lower than 1 (Fig. 5c), indicating that NH_4^+ is completely neutralized by SO_4^{2-} and NO_3^- , and there are excesses SO_4^{2-} or NO_3^- in other forms. The weak linear regression correlations were existed in $[\text{Ca}^{2+}]$ vs $[\text{SO}_4^{2-}]$ ($R^2 = 0.39$) and $[\text{Ca}^{2+}]$ vs $[\text{NO}_3^-]$ ($R^2 = 0.40$) indicate that CaSO_4 and $\text{Ca}(\text{NO}_3)_2$ also the existence form of SO_4^{2-} , NO_3^- and Ca^{2+} (Zhou et al., 2018). These compounds may come from primary emissions of soil dust. The CE was linear related to AE, and most of samples were below the 1:1 line (Fig. 5d). There are some organic acids (such as methanoic acid, acetic acid and so on) in the $\text{PM}_{2.5}$ species are not listed in our results, which may be the reason for the deficiency of anion in $\text{PM}_{2.5}$.

4.5. Transformation efficiency of the SO_4^{2-} and NO_3^-

In this study, the SOR was higher than the NOR (Fig. 3a and b), which indicates that the secondary formation of SO_4^{2-} from SO_2 strongly occurred in Kunming compared to that of NO_3^- from NO_2 (Khoder, 2002; Zhao et al., 2011) as discussed in Section 4.2.1. The NO_x and SO_2 are the precursor gases that form sulfates and nitrates, so the concentration of NO_x and SO_2 are the dominant controlling factors for SOR and NOR (Shen et al., 2009; Zhao et al., 2011; Li et al., 2013). SOR and NOR were strongly lineal related to NH_4^+ concentrations (Fig. 6) and $(\text{NH}_4)_2\text{SO}_4$ and NH_4NO_3 were main existence form for SO_4^{2-} and NO_3^- (Fig. 5a and b), which indicate that the NH_3 concentrations may be also an important controlling factors for the transformation of SO_2 and NO_2 . Seasonally, the average SOR was high in February, March and April when the O_3 concentration was high (Fig. 2c, 3a and 6a). This indicates that the higher O_3 concentrations are favorable for formation of SO_4^{2-} that was consistent with previous studies (Wang et al., 2015; Meng et al., 2016). Previous studies also suggested that the high RH would result in the high SOR values, because the humid aerosol surface was favorable for formation of SO_4^{2-} (Xu et al., 2017b). However, in our result, when the SOR was high, the RH was lower than other

months. This indicates that O_3 concentration have a greater influence on SOR than the influence of RH on SOR in Kunming. The average NOR was low in hot months, and the temperature was negatively related ($R^2 = -0.52$) with the NOR in different month (Fig. 6b), which indicate that temperature have greater influence on NOR. NO_3^- is more volatile in hot months that is the reason for NOR is more sensitive to the temperature in Kunming.

4.6. Comparison of the WSIs in Kunming with other cities and regions

The WSIs concentrations of different cities and regions around China and the world are shown in Fig. 7 and Table S1. In these cities and regions, we chose the Qinghai-Tibet Plateau and Xishan Forest Park of Kunming as two background sites where the influence of human activities on aerosols is relatively small (Xu et al., 2014; Bi, 2015). It can be seen that the concentrations of WSIs in Kunming are obviously higher than the two background sites, especially the secondary ions such as NO_3^- and NH_4^+ (Table S1). For example, the proportion of NO_3^- (3.6% and 13.3%) and NH_4^+ (7.9% and 6.7%) in total WSIs in two background sites are lower than that of Kunming (16.1% for NO_3^- and 16.7% for NH_4^+), which indicates that the influence of anthropogenic pollutants on WSIs are significant in Kunming. While the proportion of Ca^{2+} (18.6% and 20.0%) in two background sites is higher than that of Kunming (14.7%), which indicates that the input of soil dust to the WSIs is important in background sites. It could be seen clearly that the WSIs pollution is more serious in northern than southern cities in China (Fig. 7). This phenomenon may be attributed to these northern cities consume a lot of coal for heating in winter. Compared with other regions of the world, the WSIs concentrations in China are generally higher, which shows more serious aerosol pollution in China. The proportion of SNA to total WSIs (77%) in Kunming is closed to that of other cities and region. This indicates that SNA is still the main components of WSIs around the world. In SNA, the proportion of SO_4^{2-} and NO_3^- are variable and NH_4^+ is relatively stable around the world (Fig. 7 and Table S1). This result is related to the differences in emission sources to SO_4^{2-} and NO_3^- in different cities. We used the mole ratio of NO_3^- to SO_4^{2-} ($\text{NO}_3^-/\text{SO}_4^{2-}$) to express the difference of ion source in different cities (Fig. S2). In generally, high $\text{NO}_3^-/\text{SO}_4^{2-}$ (> 1) indicated that the predominance of vehicle exhaust over coal combustion sources (Kato, 1996; Wang et al., 2006; Zhang et al., 2018). It could be seen that the $\text{NO}_3^-/\text{SO}_4^{2-}$ values are lower (< 0.8) in some coastal cities, plateau region and some north cities of China, while are higher (> 0.8) in other cities. The $\text{NO}_3^-/\text{SO}_4^{2-}$ values are low in coastal cities which may be attributed to the contribution of

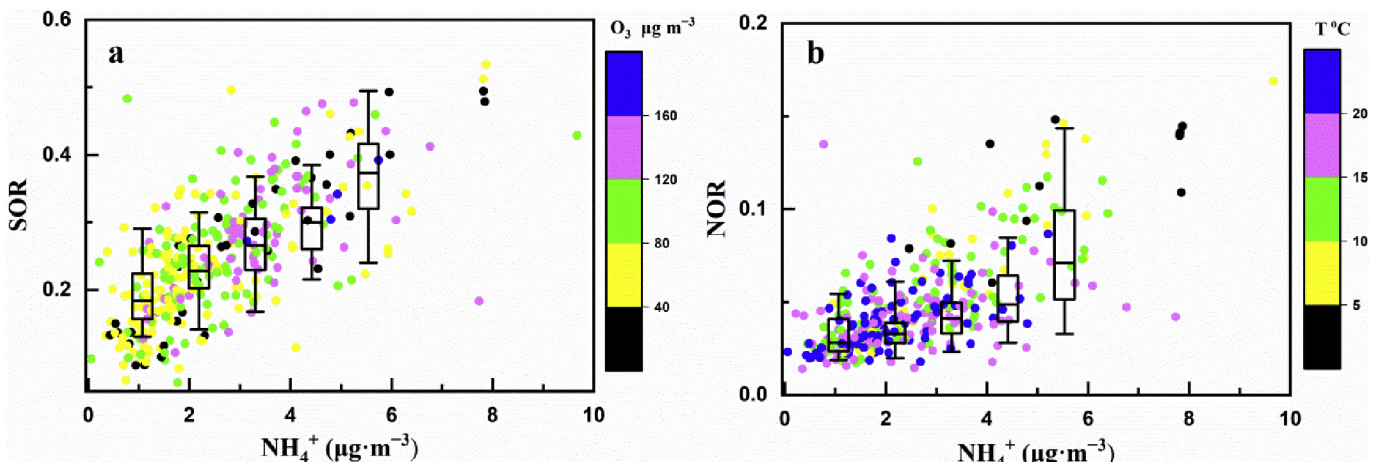


Fig. 6. Relationship between NH_4^+ and SOR, NH_4^+ and NOR, and color-coded by O_3 concentrations and Temperature (a and b), respectively. The SOR and NOR data were also binned according to NH_4^+ concentrations, respectively. For each box plot of SOR and NOR, the centerline represents the median, the box encompasses the 25th to 75th percentiles, and the bar denote the 5th and 95th percentiles.

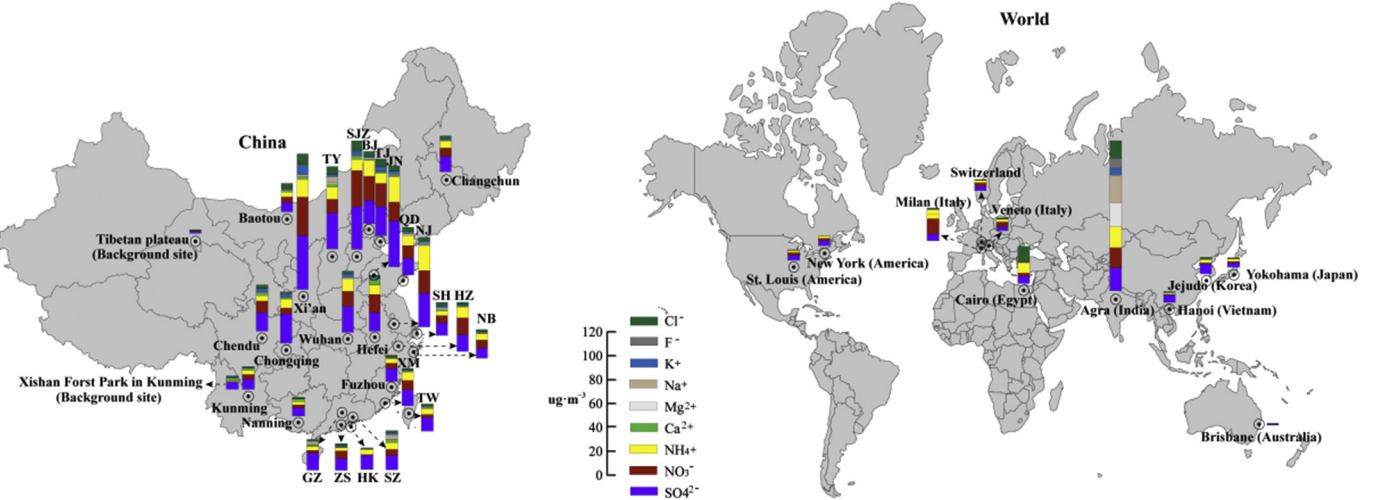


Fig. 7. Comparisons of WSIs in $\text{PM}_{2.5}$ at Kunming with other cities (regions) in China and world. The unit is $\mu\text{g}\cdot\text{m}^{-3}$. The abbreviation corresponding to the city name: TY-Taiyuan, SJZ-Shijiazhuang, BJ-Beijing, TJ-Tianjin, JN-Jinan, QD-Qingdao, NJ-Nanjing, SH-Shanghai, HZ-Hangzhou, NB-Ningbo, XM-Xiamen, TW-Taiwan, GZ-Guangzhou, ZS-Zhongshan, HK-Hongkong, SZ-Shenzhen. The data and corresponding references are supplemented in Table S1 (Supporting Information).

marine aerosol to SO_4^{2-} (Khan et al., 2010; Tao et al., 2012). In plateau regions, the high transformation efficiency of SO_4^{2-} (related to intense solar radiation) and volatilization of NO_3^- in hot months, which could result in the low $\text{NO}_3^-/\text{SO}_4^{2-}$ values. The contribution of coal combustion is more than vehicle exhaust that is the reason for low ratios in some north cities of China, such as Jinan, Taiyuan and Chongqing (He et al., 2012; He et al., 2017). The $\text{NO}_3^-/\text{SO}_4^{2-}$ values are much higher than 1 in Beijing, Hefei and Hangzhou that may because the contribution of vehicle exhaust is increased (Yang et al., 2015; Deng et al., 2016). In Veneto and Milan of Italy, the $\text{NO}_3^-/\text{SO}_4^{2-}$ values are higher than other cities which are attributed to that there is additional NO_x emission from domestic heating in Veneto and Milan (Lonati et al., 2005; Stefania et al., 2012). In Agra of India, in addition to SNA, other ions such as Ca^{2+} , Mg^{2+} , Na^+ , K^+ , F^- and Cl^- are also high (Fig. 8), this indicates that the contributions of soil dust, wood and biomass burning are important in this region (Kulshrestha et al., 2009). The Cl^- concentration were the highest in Cairo of Egypt (Table S1), which mainly emitted from the textile factories that use chlorine products for bleaching cotton (Mahmoud et al., 2002).

5. Conclusions

- (1) The WSIs are the main pollutant in $\text{PM}_{2.5}$ in Kunming, these ions are mainly from secondary aerosols, soil dust, coal combustion (primary emission), biomass burning and industry emissions. In these sources, secondary aerosols that from coal combustion, agricultural activities and vehicle exhaust contributing > 50% to $\text{PM}_{2.5}$. Seasonally, high volatility of the SNA and washout effects of rainfall in hot months (wet season) are favorable for the decreased of pollutions, while high emission, poor dispersion conditions and low removal rate are favorable for the increased of pollutions in cold months (dry season).
- (2) In addition to the concentration of SO_2 and NO_x , NH_3 concentration, solar radiation (include O_3 concentration) and temperature are also important factors affecting the concentration of secondary aerosols in Kunming. Adequate NH_3 and intense solar radiation promotes the photochemical reactions of SO_2 , NO_x and NH_3 to form NH_4HSO_4 , $(\text{NH}_4)_2\text{SO}_4$ and NH_4NO_3 . High temperature in hot months would promote the volatilization of NH_4NO_3 .

Acknowledgements

This work was supported by the Natural Science Foundation of China (grant 41863002), Open Foundation of State Key Laboratory of Loess and Quaternary Geology, Institute of Earth Environment, CAS (SKLLQG1705) and Jiangxi Province Education Department Science and Technology Research Project (GJJ170468).

Appendix A. Supplementary data

Supplementary data to this article can be found online at <https://doi.org/10.1016/j.atmosres.2019.104687>.

References

- Bi, L.M., 2015. The Pollution Characteristics of $\text{PM}_{2.5}$ and the Correlation Analysis of Meteorological Condition in Plateau City of Kunming. in Chinese. Kunming University of Science and Technology.
- Boredy, S.K.R., Kawamura, K., Bikkina, S., et al., 2016. Hygroscopic growth of particles nebulized from water-soluble extracts of $\text{PM}_{2.5}$ aerosols over the Bay of Bengal: influence of heterogeneity in air masses and formation pathways. *Sci. Total Environ.* 544, 661–669.
- Contini, D., Cesari, D., Genga, A., et al., 2014. Source apportionment of size-segregated atmospheric particles based on the major water-soluble components in Lecce (Italy). *Sci. Total Environ.* 472, 248–261.
- Dai, W., Gao, J., Cao, G., et al., 2013. Chemical composition and source identification of $\text{PM}_{2.5}$ in the suburb of Shenzhen, China. *Atmos. Res.* 2013 (122), 391–400.
- Deng, X.L., Shi, C.E., Wu, B.W., et al., 2016. Characteristics of the water-soluble components of aerosol particles in Hefei, China. *J. Environ. Sci.* 42, 32–40.
- Gao, X., Yang, L., Cheng, S., et al., 2011. Semi-continuous measurement of water-soluble ions in $\text{PM}_{2.5}$ in Jinan, China: Temporal variations and source apportionments. *Atmos. Environ.* 45, 6048–6056.
- He, K., Zhao, Q.Q., M., Y., et al., 2012. Spatial and seasonal variability of $\text{PM}_{2.5}$ acidity at two Chinese megacities: insights into the formation of secondary inorganic aerosols. *Atmos. Chem. Phys.* 12, 1377–1395.
- He, Q.S., Yan, Y.L., Guo, L.L., et al., 2017. Characterization and source analysis of water-soluble inorganic ionic species in $\text{PM}_{2.5}$ in Taiyuan city, China. *Atmos. Res.* 184, 48–55.
- Hien, P.D., Bac, V.T., Thinh, N., 2004. PMF receptor modeling of fine and coarse PM_{10} in air masses governing monsoon conditions in Hanoi, northern Vietnam. *Atmos. Environ.* 38, 189–201.
- Kalinic, N., Vladimira, V., Janko, H., et al., 1997. Fluoride mass concentration in the air at different distances from an aluminum factory. *Environ. Res.* 7–8, 253–257.
- Kato, N., 1996. Analysis of structure of energy consumption and dynamics of emission of atmospheric species related to the global environmental change (SO_x , NO_x , and CO_2) in Asia. *Atmos. Environ.* 30, 2757–2785.
- Khan, M.F., Shirasuna, Y., Hirano, K., et al., 2010. Characterization of $\text{PM}_{2.5}$, $\text{PM}_{2.5-10}$ and $\text{PM} > 10$ in ambient air, Yokohama, Japan. *Atmos. Res.* 96, 159–172.
- Khoder, M.I., 2002. Atmospheric conversion of sulfur dioxide to particulate sulfate and nitrogen nitric acid in an urban area. *Chemosphere* 49, 675–684.

- Kulshrestha, A., Bisht, D.S., Masih, J., et al., 2009. Chemical characterization of water-soluble aerosols in different residential environments of semiarid region of India. *J. Atmos. Chem.* 62, 121–138.
- Li, X.R., Wang, L.L., Ji, D.S., et al., 2013. Characterization of the size-segregated water-soluble inorganic ions in the Jing-Jin-Ji urban agglomeration: Spatial/temporal variability, size distribution and sources. *Atmos. Environ.* 77, 250–259.
- Li, J.W., Bi, L.M., Han, X.Y., et al., 2017. Characteristics and source apportionment of the water soluble inorganic ions in PM_{2.5} of Kunming (in Chinese). *J. Yunnan Univ.* 2017 (39), 63–70.
- Liu, Z., Xie, Y., Hu, B., et al., 2017. Size-resolved aerosol water-soluble ions during the summer and winter seasons in Beijing: Formation mechanisms of secondary inorganic aerosols. *Chemosphere* 183, 119–131.
- Lonati, G., Giugliano, M., Butelli, P., et al., 2005. Major chemical components of PM_{2.5} in Milan (Italy). *Atmos. Environ.* 39, 1925–1934.
- Mahmoud, A., Alan, W., Douglas, H., 2002. A preliminary apportionment of the sources of ambient PM₁₀, PM_{2.5} and VOCs in Cairo. *Atmos. Environ.* 36, 5549–5557.
- Meng, C.C., Wang, L.T., Zhang, F.F., et al., 2016. Characteristics of concentrations and water-soluble inorganic ions in PM_{2.5} in Handan City, Hebei province, China. *Atmos. Res.* 171, 133–146.
- Moller, D., 1990. The Na/Cl ration in rainwater and the sea salt chloride cycle. *Tellus B* 42B, 254–262.
- Pathak, R.K., Wu, W.S., Wang, T., 2008. Summertime PM_{2.5} ionic species in four major cities of China: nitrate formation in an ammonia-deficient atmosphere. *Atmos. Chem. Phys.* 9, 1711–1722.
- Shen, Z.X., Cao, J.J., Arimoto, R., et al., 2009. Ionic composition of TSP and PM_{2.5} during dust storms and air pollution episodes at Xi'an, China. *Atmos. Environ.* 43, 2911–2918.
- Shi, J.W., Ding, X., Zhou, Y., et al., 2016. Characteristics of chemical components in PM_{2.5} at a plateau city, Southwest China. *Frontiers of. Environ. Sci. Eng.* 10 (5), 4. <https://doi.org/10.1007/s11783-016-0841-2>.
- Stefania, S., Mauro, M., Elena, I., et al., 2012. A procedure to assess local and long-range transport contributions to PM_{2.5} and secondary inorganic aerosol. *J. Aerosol Sci.* 2012 (46), 0–76.
- Tao, J., Cheng, T., Zhang, R., et al., 2012. Chemical composition of summertime PM_{2.5} and its relationship to aerosol optical properties in Guangzhou, China. *Atmos. Ocean. Sci. Lett.* 5, 88–94.
- Tiwari, S., Pervez, S., Cinzia, P., et al., 2013. Chemical characterization of atmospheric particulate matter in Delhi, India, part II: source apportionment studies using PMF 3.0. *Sustain. Environ. Res.* 23, 295–306.
- Wang, Y., Zhuang, G.S., Zhang, X.Y., et al., 2006. The ion chemistry, seasonal cycle and sources of PM_{2.5} and TSP aerosol in Shanghai. *Atmos. Environ.* 40, 2935–2952.
- Wang, H.L., Zhu, B., Shen, L.J., et al., 2015. Water-soluble ions in atmospheric aerosols measured in five sites in the Yangtze River Delta, China: Size-fractionated, Seasonal variations and sources. *Atmos. Environ.* 2015 (123), 370–379.
- Wang, H.L., An, J.L., Cheng, M.T., et al., 2016. One year online measurements of water-soluble ions at the industrially polluted town of Nanjing, China: sources, seasonal and diurnal variations. *Chemosphere* 148, 526–536.
- Wang, J., Zhang, J.S., Liu, Z.J., et al., 2017. Characterization of chemical compositions in size-segregated atmospheric particles during severe haze episodes in three megacities of China. *Atmos. Res.* 187, 138–146.
- Xiao, H.W., Xiao, H.Y., Luo, L., et al., 2016. Atmospheric aerosol compositions over the South China Sea: temporal/variability and source apportionment. *Atmos. Chem. Phys. Discuss.* 17, 3199–3214.
- Xu, L.L., Chen, X.Q., Chen, J.S., et al., 2012. Seasonal variations and chemical compositions of PM_{2.5} aerosol in the urban area of Fuzhou, China. *Atmos. Res.* 104–105, 264–272.
- Xu, J.Z., Wang, Z.B., Yu, G.M., et al., 2014. Characteristics of water soluble ionic species in fine particles from a high altitude site on the northern boundary of Tibetan plateau: mixture of mineral dust and anthropogenic aerosol. *Atmos. Res.* 143, 43–56.
- Xu, J.S., Xu, M.X., Snape, C., et al., 2017a. Temporal and spatial variation in major ion chemistry and source identification of secondary inorganic aerosols in Northern Zhejiang Province, China. *Chemosphere* 179, 316–330.
- Xu, L.L., Duan, F.K., He, K.B., et al., 2017b. Characteristics of the secondary water-soluble ions in a typical autumn haze in Beijing. *Environ. Pollut.* 227, 296–305.
- Yang, D.Y., Liu, B.X., Zhang, D.W., et al., 2015. Correlation, Seasonal and Temporal Variation of Water-soluble Ions of PM_{2.5} in Beijing during 2012–2013 (in Chinese). *Environmental. Science.* 36, 768–773.
- Yang, Y.J., Zhou, R., Yu, Y., et al., 2017. Size-resolved aerosol water-soluble ions at a regional background station of Beijing, Tianjin, and Hebei, North China. *J. Environ. Sci.* 55, 146–156.
- Yuan, C.S., Lee, C.G., Liu, S.H., et al., 2006. Correlation of atmospheric visibility with chemical composition of Kaohsiung aerosols. *Atmos. Res.* 82, 663–679.
- Zhang, J.J., Lei, T., Huang, Z.W., et al., 2018. Seasonal variation and size distributions of water-soluble inorganic ions and carbonaceous aerosols at a coastal site in Ningbo, China. *Sci. Total Environ.* 639, 793–803.
- Zhao, J.P., Zhang, F.W., Xu, Y., et al., 2011. Characterization of water-soluble inorganic ions in size-segregated aerosols in coastal city, Xiamen. *Atmos. Res.* 2011 (99), 546–562.
- Zhao, P.S., Dong, F., He, D., et al., 2013. Characteristics of concentrations and chemical compositions for PM_{2.5} in the region of Beijing, Tianjin, and Hebei, China. *Atmos. Chem. Phys.* 2013 (13), 4631–4644.
- Zhou, J., Xing, Z., Deng, J., et al., 2016. Characterizing and sourcing ambient PM_{2.5} over key emission regions in China I: Water-soluble ions and carbonaceous fractions. *Atmos. Environ.* 135, 20–30.
- Zhou, H., Lu, C.W., He, J., et al., 2018. Stoichiometry of water-soluble ions in PM_{2.5}: Application in source apportionment for a typical industrial city in semi-arid region, Northwest China. *Atmos. Res.* 204, 149–160.
- Zhu, J., Xia, X., Che, H., et al., 2016. Study of aerosol optical properties at Kunming in Southwest China and long-range transport of biomass burning aerosols from North Burma. *Atmos. Res.* 169, 237–247.